Biosensors and Bioelectronics 25 (2010) 2283–2289

Contents lists available at ScienceDirect

Biosensors and Bioelectronics

journal homepage: www.elsevier.com/locate/bios

A molecular paramagnetic spin-doped biopolymeric oxygen sensor

Guruguhan Meenakshisundaram[a,b], Edward Eteshola[a,c], Aharon Blank[d], Stephen C. Lee[a,c], Periannan Kuppusamy[a,b,*]

[a] Davis Heart and Lung Research Institute, The Ohio State University, Columbus, OH 43210, USA
[b] Department of Internal Medicine, The Ohio State University, Columbus, OH 43210, USA
[c] Department of Biomedical Engineering, The Ohio State University, Columbus, OH 43210, USA
[d] Schulich Faculty of Chemistry, Technion - Israel Institute of Technology, Haifa 32000, Israel

ARTICLE INFO

Article history:
Received 31 December 2009
Received in revised form 1 March 2010
Accepted 8 March 2010
Available online 15 March 2010

Keywords:
EPR
Oximetry
Oxygen sensor
Trityl radical
Spin-doping
PDMS

ABSTRACT

Electron paramagnetic resonance (EPR) oximetry is a powerful technique capable of providing accurate, reliable, and repeated measurements of tissue oxygenation, which is crucial to the diagnosis and treatment of several pathophysiological conditions. Measurement of tissue pO_2 by EPR involves the use of paramagnetic, oxygen-sensitive probes, which can be either soluble (molecular) in nature or insoluble paramagnetic materials. Development of innovative strategies to enhance the biocompatibility and *in vivo* application of these oxygen-sensing probes is crucial to the growth and clinical applicability of EPR oximetry. Recent research efforts have aimed at encapsulating particulate probes in bioinert polymers for the development of biocompatible EPR probes. In this study, we have developed novel EPR oximetry probes, called perchlorotriphenylmethyl triester (PTM-TE):polydimethyl siloxane (PDMS) chips, by dissolving and incorporating the soluble (molecular) EPR probe, PTM-TE, in an oxygen-permeable polymer matrix, PDMS. We demonstrate that such incorporation (doping) of PTM-TE in PDMS enhanced its oxygen sensitivity several fold. The cast-molding method of fabricating chips enabled them to be made with increasing amounts of PTM-TE (spin density). Characterization of the spin distribution within the PDMS matrix, using EPR micro-imaging, revealed potential inhomogeneties, albeit with no adverse effect on the oxygen-sensing characteristics of PTM-TE:PDMS. The chips were resistant to autoclaving or *in vitro* oxidoreductant treatment, thus exhibiting excellent *in vitro* biostability. Our results establish PTM-TE:PDMS as a viable probe for biological oxygen-sensing, and also validate the incorporation of soluble probes in polymer matrices as an innovative approach to the development of novel probes for EPR oximetry.

1. Introduction

Oxygen is the primary source of energy for all aerobic life, including human. Insufficient oxygen means insufficient biological energy, which can lead to a number of complications ranging from mild fatigue to life-threatening disease. Given the critical role that oxygen plays in the maintenance of good health, the measurement of oxygen (oximetry) in various tissues and organs of the body assumes primary importance, especially under pathophysiological conditions. Of the several methods for oximetry (Springett and Swartz, 2007; Vikram et al., 2007), electron paramagnetic resonance (EPR) oximetry, has a unique advantage in its ability to measure absolute oxygen concentration (Khan et al., 2007c). The technique is also capable of making minimally invasive, real-time (*in vivo*), and repeated measurements of oxygen partial pressure (pO_2) in tissues.

EPR has been employed extensively for both *in vitro*, as well as, *in vivo* oximetry. The technique has been used for several *in vitro* studies to monitor intracellular and extracellular oxygen levels, cellular respiration, as well, as oxygen consumption (Kutala et al., 2004; Pandian et al., 2005, 2003a; Presley et al., 2006). Oximetry using EPR has also been applied to a wide variety of tissues, including tumors, brain, heart, skeletal, muscle, liver, kidney, and the skin (Swartz and Clarkson, 1998). Of special mention are the cardiac applications of EPR oximetry. The role of cardio-protective agents against ischemia–reperfusion injury has been studied extensively using EPR oximetry (Khan et al., in press, 2007b; Mohan et al., 2009). In recent work, the method has been used to study the role of oxygen in stem cell therapy for ischemic heart disease, and to establish improvement in myocardial oxygenation due to stem-cell therapy (Chacko et al., 2009; Khan et al., 2007a). Further, preconditioning of stem cells using pharmacological agents or hyperbaric oxygenation therapy has also been evaluated using EPR oximetry (Khan et al., 2009; Wisel et al., 2009).

* Corresponding author at: The Ohio State University, 420 West 12th Avenue, Room 114, Columbus, OH 43210, USA. Tel.: +1 614 292 8998; fax: +1 614 292 8454.
E-mail address: kuppusamy1@osu.edu (P. Kuppusamy).

0956-5663/$ – see front matter © 2010 Elsevier B.V. All rights reserved.
doi:10.1016/j.bios.2010.03.011

The measurement of oxygen using EPR is rendered possible by the use of paramagnetic probes, whose EPR spectral characteristics are sensitive to changes in molecular oxygen in the local environment. There are two classes of paramagnetic probes that are sensitive to oxygen: soluble (molecular) probes, such as nitroxyls and triarylmethyl (trityl) radicals, and insoluble particulate materials, such as lithium phthalocyanine (LiPc) and its derivatives, namely lithium naphthalocyanine (LiNc) and lithium octa-*n*-butoxy naphthalocyanine (LiNc-BuO) (Ilangovan et al., 2002; Liu et al., 1993; Pandian et al., 2003b; Swartz and Clarkson, 1998). The direct use these oxygen-sensitive probes for *in vivo* applications has been hindered by a few crucial concerns: soluble probes suffer from relatively low sensitivity to oxygen and the ability to measure only concentrations of dissolved oxygen, whereas particulate probes are plagued by concerns associated with their dispersion in the tissue, leading to signal loss over time, and biocompatibility concerns, due to direct tissue contact. The widespread use of EPR oximetry for clinically relevant *in vivo* applications, and its eventual clinical transformation, requires innovative approaches in EPR probe development.

To this end, previous works along these lines have focused on encapsulating insoluble particulate probes, including LiPc, LiNc, and LiNc-BuO, in biocompatible polymer matrices, such as Teflon AF 2400 (TAF) and polydimethyl siloxane (PDMS), for the development of oxygen-sensing implants or chips (Dinguizli et al., 2006; Eteshola et al., 2009; Meenakshisundaram et al., 2009a,b, 2010; Pandian et al., in press). Although a good body of work has been dedicated to the development of novel particulate probe-based approaches to EPR oximetry, soluble probes have not received much attention, primarily owing to their poor oxygen sensitivity. In the present study, we have developed a new oxygen-sensing probe, the first of its kind, by the dissolution and subsequent incorporation (doping) of a molecular EPR probe in a biocompatible polymer matrix. We have chosen perchlorotriphenylmethyl triester (PTM-TE), a trityl probe, as the soluble EPR probe and PDMS as the polymer matrix for this application. PTM-TE is well-suited for EPR oximetry, since it exhibits a single-line and narrow EPR spectrum (Dang et al., 2007). The oxygen response of PTM-TE in solution is linear, with reasonable sensitivity to changes in oxygen. We chose PDMS as the polymer for this application based on its excellent oxygen-permeability, biocompatibility (Belanger and Marois, 2001; Mata et al., 2005), and our previous successful attempts at using this polymer as the matrix for the fabrication of particulate EPR probe-based implantable oxygen-sensing chips (Meenakshisundaram et al., 2009a,b, 2010).

We have exploited the non-polar nature of PTM-TE and the hydrophobic nature of PDMS to dissolve, and incorporate, PTM-TE molecules in the PDMS matrix, for the development of oxygen-sensitive chips, denoted as PTM-TE:PDMS chips. We report the fabrication and *in vitro* characterization of this new hybrid material, including oxygen response/sensitivity, density/distribution of PTM-TE molecules in the PDMS matrix, and *in vitro* biostability. The study demonstrated that the incorporation of PTM-TE in PDMS enhanced its oxygen sensitivity, and confirmed the success of our approach for the development of novel oxygen sensors using soluble EPR probes.

2. Materials and methods

2.1. Materials

PTM-TE was synthesized, in powder form, as reported (Dang et al., 2007), while PDMS was procured from Dow Corning (Midland, MI) as medical grade Silastic (MDX4-4210). Dimethyl sulfoxide (DMSO), hydrogen peroxide (H_2O_2), and glutathione (GSH) were obtained from Sigma–Aldrich (St. Louis, MO). S-nitroso-N-acetyl penicillamine (SNAP) was obtained from Invitrogen (Eugene, OR).

2.2. Fabrication of PTM-TE:PDMS chips

Fabrication of PTM-TE:PDMS chips was carried out by cast-molding and polymerization as described (Meenakshisundaram et al., 2009a). In brief, PTM-TE was mixed thoroughly, and allowed to dissolve, in the uncured PDMS base-catalyst mixture. Subsequently, this mixture was cured at 75 °C for 7 h resulting in the formation of a large PTM-TE:PDMS chip. Smaller pieces of various sizes (from 0.5 to 2 mm) were cut from the larger chip and used for testing. Four different formulations of PTM-TE:PDMS were fabricated by dissolving different amounts of PTM-TE powder (5, 10, 15, and 20 mg) in the same amount of PDMS (6 g). The resultant formulations were denoted as F-5, F-10, F-15, and F-20, with the suffix (number) denoting the amount of PTM-TE used.

2.3. Evaluation of oxygen response (calibration) and spin density

X-band (9.8 GHz) EPR spectrometry was used to evaluate the oxygen calibration and spin density of PTM-TE:PDMS chips, as described (Meenakshisundaram et al., 2009a). For comparison of oxygen calibration with PTM-TE:PDMS chips, a solution of PTM-TE in DMSO (100 μM) was used. The spin density of PTM-TE:PDMS chips was calculated by comparing the area under the curve (AUC) of the chips with the AUC of a known spin density standard, triarylmethyl radical (TAM) (Kutala et al., 2004).

2.4. EPR micro-imaging

EPR micro-imaging was performed on a custom-built EPR microscope at the Technion—Israel Institute of Technology (Haifa, Israel). The design of this system was adapted from the EPR microscope at Cornell University (Ithaca, NY) (Blank et al., 2004), with some upgrades made to the imaging probe and the spectrometer hardware (Blank et al., 2009). Sample preparation for micro-imaging involved slicing a larger piece of PTM-TE:PDMS using a sharp scalpel to approximately 100-μm slices, which were further cut to a shape of an equilateral triangle with a side dimension of ~500 μm, to fit into the imaging probe of the microscope. Samples were made anoxic by sealing them in a specially prepared glass sample holder under argon atmosphere (Halevy et al., 2007). A 2-D spatial 1-D spectral image of the prepared sample was acquired using the following parameters: 128 spatial projections × 32 spectral projections (total of 4096 projections); 128 points per projection; time constant, 0.1 s; modulation amplitude, 0.27 G; maximum gradient magnitude of 4.9 T/m for the *X*-axis and 4.5 T/m for the *Y*-axis; microwave frequency, 15.46 GHz.

2.5. Autoclaving and oxidoreductant treatment

A bench-top analog sterilizer (Tuttnauer® by Brinkmann Instruments, New York) was used to autoclave PTM-TE:PDMS chips. Autoclaving was performed at the following settings: 121 °C for 1 h at 1 atm pressure (wet cycle using steam), followed by exhaust-drying for 15–20 min. PTM-TE:PDMS chips were treated *in vitro* with common biological oxidoreductants in order to evaluate their biostability. The following oxidants and reductants were used as described: nitric oxide, produced using a 5-mM solution of SNAP in distilled water; 1-mM H_2O_2; and GSH in distilled water (5 mM). Chips were immersed in solutions of the oxidoreductants for 30 minutes, and subsequently air-dried for 60 min, following which oxygen-calibration and spin-density measurements were made. PTM-TE:PDMS chips that were not autoclaved or subjected

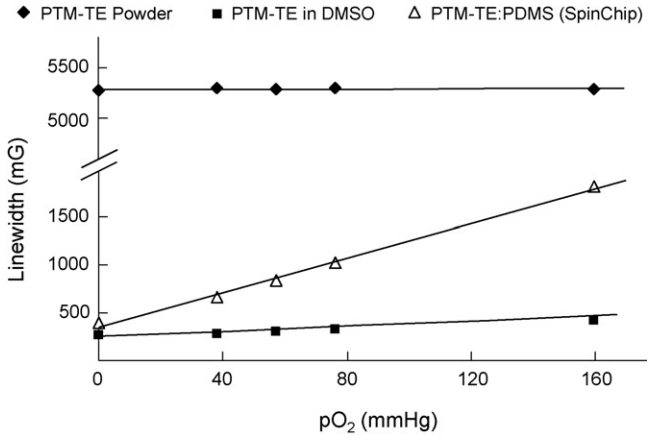

Fig. 1. Effect of the incorporation of PTM-TE in PDMS on its oxygen sensitivity. Analysis of the oxygen calibration curves of PTM-TE powder, PTM-TE dissolved in DMSO, and PTM-TE incorporated in PDMS revealed that the PTM-TE powder was not sensitive to oxygen, exhibiting a steady linewidth of approximately 5.3 G. PTM-TE dissolved in DMSO exhibited a linear calibration with a sensitivity of 1.0 ± 0.1 mG/mm Hg. The calibration curve for PTM-TE:PDMS was also linear with an oxygen sensitivity of 9.1 ± 0.2 mG/mm Hg. Data demonstrate that the incorporation of PTM-TE in the PDMS matrix enabled significant enhancement of its oxygen sensitivity. Data are represented as mean ± SD ($n = 3$).

to treatment with oxidoreductants were used as controls for comparison with treated chips.

2.6. Statistical analysis

Data were expressed as mean ± SD and compared using a Student's *t*-test, with the level of significance (p) set at 0.05.

3. Results and discussion

3.1. Effect of the incorporation of PTM-TE in PDMS on its oxygen sensitivity

The EPR spectrum of solid PTM-TE is not sensitive to molecular oxygen, and hence cannot be used in its native form for oxygen-sensing applications. In addition, PTM-TE is insoluble in water. In order to compare with PTM-TE:PDMS chips, and to determine the effect of PTM-TE incorporation in PDMS on its oxygen sensitivity, we dissolved PTM-TE in DMSO, a solvent commonly used in biological applications to dissolve non-polar compounds. PTM-TE dissolved in DMSO is oxygen-sensitive (Dang et al., 2007). However, the oxygen sensitivity of PTM-TE in DMSO was very small (~1–2 mG/mm Hg), as demonstrated previously (Dang et al., 2007), as well as, by our current results (Fig. 1).

Given the non-polar nature of PTM-TE, we rationalized that the use of a highly hydrophobic polymer, such as PDMS, for the incorporation of PTM-TE, and the fabrication of chips, would enable dissolution of the PTM-TE in the polymer, thereby rendering it oxygen sensitive. As expected, when PTM-TE was dissolved in PDMS, and further solidified into chips (PTM-TE:PDMS), we observed that the oxygen sensitivity increased almost 9-fold, compared to PTM-TE dissolved in DMSO (Fig. 1). In addition, the enhancement in sensitivity of PTM-TE, when incorporated in PDMS, was significant enough to make it comparable to the oxygen sensitivity of the particulate probe, LiNc-BuO (~8–9 mG/mm Hg) (Pandian et al., 2003b).

The incorporation of PTM-TE in the PDMS matrix enabled the probe to measure the pO_2 of the surrounding environment directly, as compared to measuring dissolved oxygen concentration (which can be converted into pO_2) when used in the form of a solution. It should also be noted that the oxygen response of PTM-TE:PDMS remained linear within the range of pO_2 tested (0–160 mm Hg). Since the pO_2 for most biological applications would fall within this range, the PTM-TE:PDMS chip can be used successfully to provide pO_2 measurements with good sensitivity.

Although, the underlying mechanism for the observed increase in sensitivity of PTM-TE when doped into PDMS is unknown, we speculate that the molecular spins of PTM-TE were arrested in the PDMS matrix, allowing for more efficient collisions (spin exchange) between molecular oxygen and the arrested spins, thereby enhancing the oxygen sensitivity. Conversely, when PTM-TE is dissolved in a solvent, the spins (molecules) would be tumbling rapidly and constantly in motion (unarrested), which may not result in as effective molecular collisions with oxygen. Further, owing to the excellent oxygen permeability of PDMS, molecular oxygen may be able to reach and interact with the incorporated spins of PTM-TE in the PDMS matrix without any hindrance, which may potentially contribute to the higher oxygen sensitivity observed.

3.2. Loading of PTM-TE in the PDMS matrix

The cast-molding and polymerization method, employed for the fabrication of PTM-TE:PDMS, was not only simple to perform on a lab bench without the need for any expensive equipment, but it also allowed for increasing amounts of PTM-TE to be incorporated into the PDMS matrix. The ability to increase the PTM-TE loading into the chips will be useful in applications that require high spin density of the probe, such as oxygen measurements in deeper tissues. The relative increase in the loading of PTM-TE in the PDMS matrix had a direct correlation with the intensity of the characteristic red color of the fabricated chips, as observed in the photograph in Fig. 2. The pictures also showed that PTM-TE:PDMS chips can be made in different sizes and shapes using the cast-molding method.

In order to verify that the increased loading did not cause spin-induced line-broadening (independent of oxygen-induced broadening), due to close packing of PTM-TE spins, we calibrated the oxygen response of the four different formulations of PTM-TE:PDMS, *viz.* F-5, F-10, F-15, and F-20 (Fig. 3). Any spin–spin broadening, due to close proximity of spins, will lead to erroneous pO_2 measurements, since the spin-induced broadening effect will be added to the actual oxygen-induced line broadening. However, the oxygen response of all the formulations was linear, with no significant difference in slope (between calibration curves) (Fig. 3). Therefore, it was evident that within the range of PTM-TE amounts loaded (up to 20 mg) into PDMS (6 g), we did not observe any spin–spin broadening effects. Further, loading 20 mg of PTM-TE in PDMS (F-20) was sufficient to provide a strong EPR signal, both *in vitro* and *in vivo* (data not shown), and hence did not necessitate the loading of more material into the matrix. However, if required by the nature of the application, and provided that there is no spin-induced broadening, the cast molding process will enable any amount of PTM-TE, within its limit of solubility in PDMS, to be loaded into the PDMS matrix.

It should be noted that the oxygen-sensing ability of the incorporated PTM-TE does not depend on the amount that is loaded into the PDMS matrix. The 5–20 mg employed in this study is a representative range. The use of higher concentrations, although may provide better signal-to-noise ratio (SNR), is limited by solubility of the spin probe in the polymer and possible spin–spin broadening. The formulation F-20 was the optimum choice for experimentation and analysis, since it provided the best SNR.

3.3. Spin distribution within PTM-TE:PDMS chips

EPR micro-imaging was used to evaluate the distribution of PTM-TE spins within the PDMS matrix. All the micro-imaging

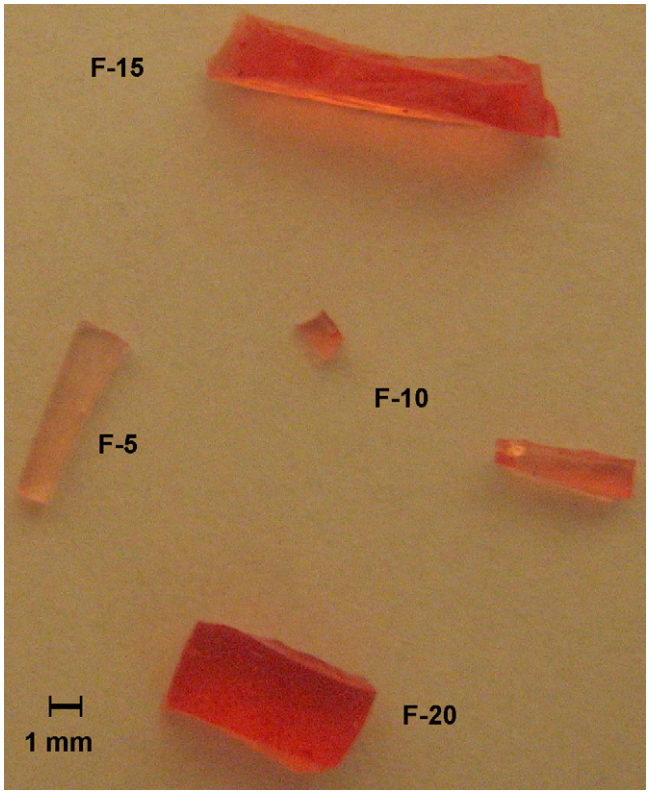

Fig. 2. PTM-TE:PDMS formulations. Photograph of the four PTM-TE:PDMS formulations, made by cast-molding and polymerization, with four different amounts of PTM-TE (5, 10, 15, and 20 mg), each incorporated into 6 g of PDMS. Photograph shows an increase in the intensity of the color (red), which directly correlated to the increase in the amount of PTM-TE that was used for making the different formulations. Results indicate successful incorporation of increased PTM-TE spins in the PDMS matrix. (For interpretation of the references to color in this figure legend, the reader is referred to the web version of the article.)

experiments were performed at a frequency of 15.46 GHz, and PTM-TE:PDMS chips made with 20 mg of PTM-TE in 6 g of PDMS (formulation F-20) were used. The sample was chosen to contain a small solid cluster of PTM-TE spins in the size of a few tens of a micrometer, which was apparent under an optical microscope (Fig. 4(a)). The EPR micro-imaging probe employed a millimeter-size resonator operating at relatively high frequency. Under these conditions the EPR spectral properties of the small sample of PTM-TE:PDMS could be measured with high spectral resolution. As a result, it can be observed that the first-derivative EPR spectrum of PTM-TE:PDMS (under anoxic condition) has two components (Fig. 4(b)), a sharper line riding on top of a broader line. The presence of two spectral components may be attributed to the incomplete dissolution of PTM-TE in PDMS, potentially leading to the presence of dissolved (oxygen-sensitive) regions of PTM-TE, and undissolved (oxygen-insensitive) clusters of PTM-TE, within the PDMS matrix. The oxygen-insensitive clusters would be responsible for the broader component of the composite spectrum, whereas the oxygen-sensitive regions would contribute to the sharper line. With the introduction of molecular oxygen, by flushing the sample with a known concentration of oxygen, the two components merged to give one spectrum (data not shown), indicating oxygen-induced broadening of the sharper, oxygen-sensitive spectral component.

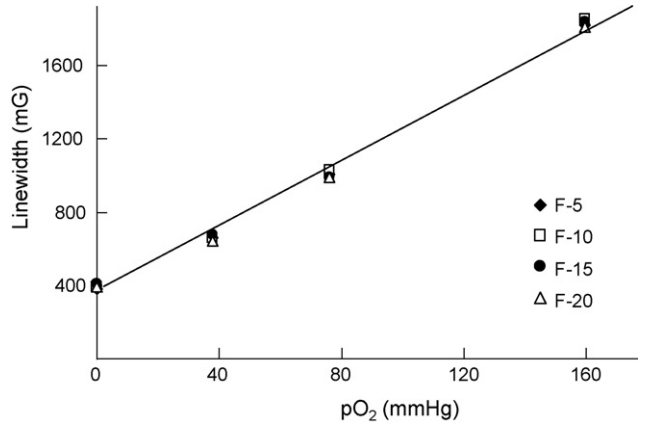

Fig. 3. Oxygen calibration of the PTM-TE:PDMS formulations. Each of the four formulations of PTM-TE:PDMS exhibited a linear O_2 calibration, evaluated using X-band EPR spectroscopy, with comparable slopes (oxygen sensitivities). Results (mean ± SD, $n = 3$) indicate that the increased amount of PTM-TE spins in the different formulations did not result in any spin-induced line-broadening (up to the 20 mg amount tested), and any resultant shift in the oxygen calibration.

Similar presence of multiple components was observed in the 2-D spatial 1-D spectral image of PTM-TE:PDMS obtained using the EPR microscope (Fig. 4(c)). Spatial imaging, compared to single spectral analysis, showed the presence of multiple regions of varying spectral linewidths, as shown in the spatially resolved spectrum plot (Fig. 4(d)). The sharper lines corresponded to regions of dissolved (oxygen-sensitive) PTM-TE (in PDMS), thus characterized by the small linewidth (anoxic condition), while the broader (flatter) spectral components corresponded to undissolved, oxygen-insensitive clusters.

It must be noted that at the operational frequencies of X-band (9.8 GHz) and L-band (1.2 GHz), which have been used for the rest of the experiments in this study, such spectral separation (as with the 15.4 GHz) was not observed, since the frequency was not sufficient to provide such high spectral resolution. In addition, the relative amount of PTM-TE spins in the form of clusters may have been lesser in the macroscopic samples used for the experiments at X-band or L-band, compared to the microscopic samples prepared for micro-imaging studies. As a result, the spectral separation, due to the presence of clusters, may not have been observed with the X- or L-band experiments. Further, it is of crucial importance to note that irrespective of the possible presence of two spectral components, the oxygen calibration of PTM-TE:PDMS remained linear (Figs. 1 and 3), even under extreme conditions of sterilization and chemical treatment (Fig. 5). Therefore, the oxygen-sensing ability of PTM-TE:PDMS was not compromised in the range of pO_2 tested (0–160 mm Hg) and at the EPR frequencies employed (X- or L-band).

3.4. *In vitro biostability of PTM-TE:PDMS*

In order to characterize the *in vitro* performance of PTM-TE:PDMS chips, and to evaluate their biostability prior to preliminary *in vivo* testing (presented as supplementary information), we subjected them to sterilization by autoclaving or treatment with common biological oxidizing and reducing agents. Since, the chips were intended for biological application, we evaluated the change in their oxygen-sensing response, if any, to sterilization, which is crucial to avoid bacterial infection, as well as, to oxidoreductant treatment, as an indicator of the ability of these chips to survive the redox environment *in vivo* (when implanted).

Results showed that the oxygen sensing ability, in terms of the linearity of the calibration (Fig. 5), as well as, the spin density (Fig. 6) of these chips was not affected significantly by sterilization or oxidoreductant treatment. In addition, the oxygen sensitivities of PTM-TE:PDMS samples that were autoclaved (7.6 ± 0.2 mG/mm Hg), or treated with the following oxidoreductants; H_2O_2 (8.2 ± 0.2 mG/mm Hg), NO (8.6 ± 0.5 mG/mm Hg) or

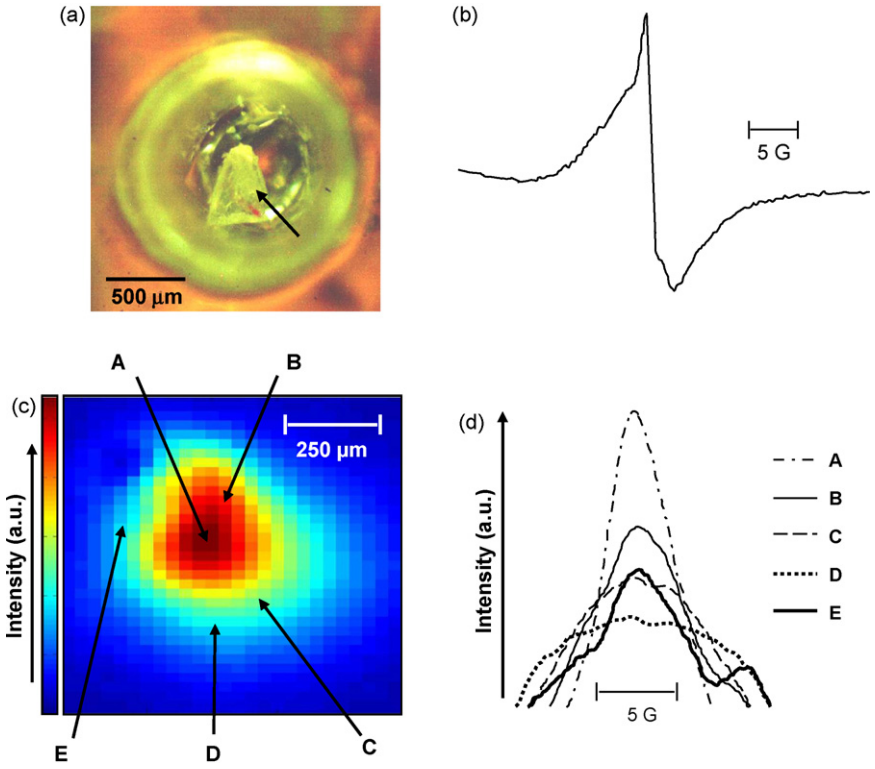

Fig. 4. Spin distribution within PTM-TE:PDMS chips. EPR micro-imaging was used to determine the distribution of PTM-TE spins within the PDMS matrix. PTM-TE:PDMS chips with 20 mg of PTM-TE incorporated into 6 g of PDMS (highest spin density formulation) were used for the micro-imaging experiments. (a) Optical microscope image of a PTM-TE:PDMS sample prepared for EPR micro-imaging. (b) Continuous wave (CW) EPR spectrum of the prepared PTM-TE:PDMS sample, acquired at 15.46 GHz with the micro-imaging probe (without gradients), showing the presence of two spectral components. (c) CW-EPR image of a slice of PTM-TE:PDMS. A 2-D spatial image slice (taken out of the 2-D spatial 1-D spectral image at the center of the spectrum), with the different colored regions representing concentration of PTM-TE spins within the PDMS matrix, is shown. Image resolution is ~30 μm. (d) Spatially resolved spectrum plot showing differentiation between areas with relatively narrow line (almost no clusters) and areas with broader line (mainly clusters). Representative spectra corresponding to clustered and non-clustered areas within the sample have also been denoted in the 2-D spatial image slice shown in (b). Results indicate that the distribution of PTM-TE spins within the PDMS matrix was non-uniform, which did not, however, affect the oxygen sensing ability of ×these chips.

GSH (8.4 ± 0.3 mG/mm Hg), were not significantly different from that of control samples (8.2 ± 0.4 mG/mm Hg). The fact that the oxygen calibration and sensitivity, as well as, spin density remained intact, after exposure to high temperature/pressure conditions in the autoclave or after being exposed to high concentrations of potent oxidizing and reducing agents, indicated that the polymer and the incorporated PTM-TE molecules were both resistant to either treatment. Any change in the properties of the polymer could have led to loss of oxygen permeability, and a subsequent change in oxygen-sensing characteristics of the incorporated PTM-TE spins, which, however, was not observed. In addition, the incorporated PTM-TE molecules also retained their paramagnetism, in the face of harsh physical and chemical (redox) conditions. Further, in order to verify if the pH of the medium/solution had any influence on the performance of PTM-TE:PDMS chips, we carried out EPR detection experiments before and after immersion of these chips in buffer solutions, ranging in pH from 4.3 (acidic) to 9.3 (basic). Results (data not shown) showed that the oxygen-sensing ability of PTM-

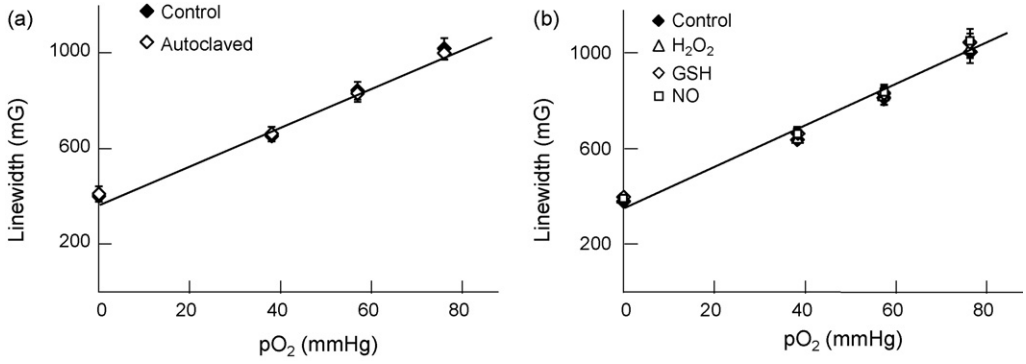

Fig. 5. Effect of sterilization and oxidoreductant treatment on the oxygen sensitivity of PTM-TE:PDMS. (a) Effect of autoclaving on the oxygen calibration of PTM-TE:PDMS. Comparison of the O_2 calibration curves of unsterilized (control) and sterilized PTM-TE:PDMS chips ($n = 3$, mean ± SD) revealed that the high temperature and pressure conditions of the autoclave did not have any significant effect on the linearity or slope of the oxygen calibration. (b) Effect of oxidoreductant treatment on the oxygen calibration of PTM-TE:PDMS. Chips ($n = 3$) were treated with biological oxidizing and reducing agents, *viz.* nitric oxide (NO), 1-mM hydrogen peroxide (H_2O_2), and 5-mM glutathione (GSH) for 30 min, and subsequently air-dried. Data ($n = 3$, mean ± SD) show that *in vitro* exposure to these oxidizing or reducing agents did not have any significant effect on the oxygen calibration of PTM-TE:PDMS.

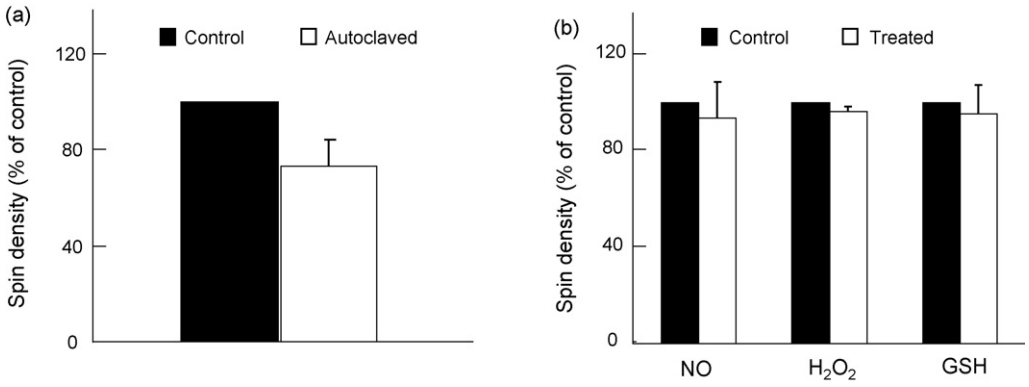

Fig. 6. Effect of sterilization and oxidoreductant treatment on the spin density of PTM-TE:PDMS. Spin density of PTM-TE:PDMS after autoclaving (a) or treatment with oxidoreductants (b). Spin density of PTM-TE:PDMS chips, before and after treatment, were estimated by comparing with the spin density of a known standard. Data ($n = 3$, mean ± SD), represented as percentage of control, show that either autoclaving or oxidoreductant treatment did not affect the spin density of PTM-TE:PDMS chips significantly.

TE:PDMS was not affected by the pH of the medium. That the oxygen calibration of oxidoreductant-treated samples was not significantly different from that of control (Fig. 5) also indicated that the pH of the solutions of oxidizing and reducing agents in which the PTM-TE:PDMS chips were immersed did not affect their sensing performance.

Although these results demonstrated the resistance of PTM-TE:PDMS chips to treatment with some powerful biological oxidoreductants, the effect of superoxide on PTM-TE:PDMS is an important consideration. It is known that superoxide reacts with neat PTM-TE and renders it EPR-inactive (Dang et al., 2007). It may be reasonable to expect that the PDMS may provide a selective barrier and protect the incorporated PTM-TE from reacting with superoxide, thereby improving the sensing selectivity to oxygen, primarily due to the excellent oxygen permeability of PDMS and the high reactivity of superoxide, which may react with some component of the PDMS matrix before reaching the incorporated PTM-TE. In the context of *in vivo* applications, especially in the short-term, we did not expect or observe any significant change in oxygen sensitivity of PTM-TE:PDMS (Supplementary Fig. S1), due to the low *in vivo* concentration of superoxide under normal physiological conditions. However, a slow reaction of superoxide with PTM-TE:PDMS over time (*in vivo*) cannot be ruled out, especially under pathophysiological conditions or due to repeated exposure of PTM-TE:PDMS to superoxide over time.

4. Summary and conclusions

We have successfully developed novel EPR oximetry sensors, PTM-TE:PDMS chips, by dissolving and incorporating an oxygen-sensitive soluble probe, PTM-TE, in a biocompatible, oxygen-permeable polymer matrix (PDMS). The chips exhibited enhanced sensitivity to oxygen, which was comparable to the sensitivity of particulate EPR probes. The cast-molding method, employed to fabricate these chips, allowed the loading of different amounts of PTM-TE in the PDMS matrix, enabling chips with increasing spin density to be made. High-frequency EPR micro-imaging revealed the possible presence of dissolved (oxygen-sensitive) and undissolved (oxygen-insensitive) regions of PTM-TE in the PDMS matrix, however, with no apparent effect on oxygen-sensing performance. PTM-TE:PDMS chips were biostable, and exhibited no significant change in linearity of oxygen calibration or spin density in response to sterilization (autoclaving) or oxidoreductant treatment. Overall, we have demonstrated a new approach for the fabrication of a novel EPR oximetry sensor using soluble EPR probes, which will serve to expand the capability and enhance the applicability of EPR for biological oximetry.

Acknowledgments

This study was supported by NIH grant EB004031, and by the US-Israel Binational Science Foundation (BSF) (grant 2005258). We thank Dr. Nasim Warwar for the preparation of samples for EPR microscopy.

Appendix A. Supplementary data

Supplementary data associated with this article can be found, in the online version, at doi:10.1016/j.bios.2010.03.011.

References

Belanger, M.C., Marois, Y., 2001. J. Biomed. Mater. Res. 58 (5), 467–477.
Blank, A., Dunnam, C.R., Borbat, P.P., Freed, J.H., 2004. Rev. Sci. Instrum. 75, 3050–3061.
Blank, A., Halevy, R., Shklyar, M., Shtirberg, L., Kuppusamy, P., 2010. J. Magn. Reson. 203, 150–155.
Chacko, S.M., Khan, M., Kuppusamy, M.L., Pandian, R.P., Varadharaj, S., Selvendiran, K., Bratasz, A., Rivera, B.K., Kuppusamy, P., 2009. Am. J. Physiol. Heart Circ. Physiol. 296 (5), H1263–H1273.
Dang, V., Wang, J., Feng, S., Buron, C., Villamena, F.A., Wang, P.G., Kuppusamy, P., 2007. Bioorg. Med. Chem. Lett. 17 (14), 4062–4065.
Dinguizli, A., Jeumont, S., Beghein, N., He, J., Walczak, T., Lesniewski, P.N., Hou, H., Grinberg, O.Y., Sucheta, A., Swartz, H.M., Gallez, B., 2006. Biosens. Bioelectron. 21 (7), 1015–1022.
Eteshola, E., Pandian, R.P., Lee, S.C., Kuppusamy, P., 2009. Biomed. Microdevices 11 (2), 379–387.
Halevy, R., Talmon, Y., Blank, A., 2007. Appl. Magn. Reson. 31, 589–596.
Ilangovan, G., Manivannan, A., Li, H.Q., Yanagi, H., Zweier, J.L., Kuppusamy, P., 2002. Free Radic. Biol. Med. 32 (2), 139–147.
Khan, M., Kutala, V.K., Vikram, D.S., Wisel, S., Chacko, S.M., Kuppusamy, M.L., Mohan, I.K., Zweier, J.L., Kwiatkowski, P., Kuppusamy, P., 2007a. Am. J. Physiol.: Heart Circul. Physiol. 293 (4), H2129–H2139.
Khan, M., Meduru, S., Mohan, I.K., Kuppusamy, M.L., Wisel, S., Kulkarni, A., Rivera, B.K., Hamlin, R.L., Kuppusamy, P., 2009. J. Mol. Cell. Cardiol. 47 (2), 275–287.
Khan, M., Meduru, S., Mostafa, M., Khan, S., Hideg, K., Kuppusamy, P. J. Pharmacol. Exp. Ther., in press.
Khan, M., Mohan, I.K., Kutala, V.K., Kumbala, D., Kuppusamy, P., 2007b. J. Pharmacol. Exp. Ther. 323 (3), 813–821.
Khan, N., Williams, B.B., Hou, H., Li, H., Swartz, H.M., 2007c. Antioxid. Redox Signal 9 (8), 1169–1182.
Kutala, V.K., Parinandi, N.L., Pandian, R.P., Kuppusamy, P., 2004. Antioxid. Redox Signal 6 (3), 597–603.
Liu, K.J., Gast, P., Moussavi, M., Norby, S.W., Vahidi, N., Walczak, T., Wu, M., Swartz, H.M., 1993. Proc. Natl. Acad. Sci. U.S.A. 90 (12), 5438–5442.
Mata, A., Fleischman, A.J., Roy, S., 2005. Biomed. Microdevices 7 (4), 281–293.
Meenakshisundaram, G., Eteshola, E., Pandian, R.P., Bratasz, A., Lee, S.C., Kuppusamy, P., 2009a. Biomed. Microdevices 11 (4), 773–782.
Meenakshisundaram, G., Eteshola, E., Pandian, R.P., Bratasz, A., Selvendiran, K., Lee, S.C., Krishna, M.C., Swartz, H.M., Kuppusamy, P., 2009b. Biomed. Microdevices 11 (4), 817–826.
Meenakshisundaram, G., Pandian, R.P., Eteshola, E., Lee, S.C., Kuppusamy, P., 2010. J. Magn. Reson. 203 (1), 185–189.
Mohan, I.K., Khan, M., Wisel, S., Selvendiran, K., Sridhar, A., Carnes, C.A., Bognar, B., Kalai, T., Hideg, K., Kuppusamy, P., 2009. Am. J. Physiol.: Heart Circul. Physiol. 296 (1), H140–H151.

Pandian, R.P., Kutala, V.K., Liaugminas, A., Parinandi, N.L., Kuppusamy, P., 2005. Mol. Cell. Biochem. 278 (1–2), 119–127.
Pandian, R.P., Kutala, V.K., Parinandi, N.L., Zweier, J.L., Kuppusamy, P., 2003a. Arch. Biochem. Biophys. 420 (1), 169–175.
Pandian, R.P., Meenakshisundaram, G., Bratasz, A., Eteshola, E., Lee, S.C., Kuppusamy, P. Biomed. Microdevices, in press.
Pandian, R.P., Parinandi, N.L., Ilangovan, G., Zweier, J.L., Kuppusamy, P., 2003b. Free Radic. Biol. Med. 35 (9), 1138–1148.
Presley, T., Kuppusamy, P., Zweier, J.L., Ilangovan, G., 2006. Biophys. J. 91 (12), 4623–4631.
Springett, R., Swartz, H.M., 2007. Antioxid. Redox Signal 9 (8), 1295–1301.
Swartz, H.M., Clarkson, R.B., 1998. Phys. Med. Biol. 43 (7), 1957–1975.
Vikram, D.S., Zweier, J.L., Kuppusamy, P., 2007. Antioxid. Redox Signal 9 (10), 1745–1756.
Wisel, S., Khan, M., Kuppusamy, M.L., Mohan, I.K., Chacko, S.M., Rivera, B.K., Sun, B.C., Hideg, K., Kuppusamy, P., 2009. J. Pharmacol. Exp. Ther. 329 (2), 543–550.